Single-nuclei transcriptomics of schizophrenia prefrontal cortex primarily implicates neuronal subtypes

Benjamin C. Reiner[1,3,*], Richard C. Crist[1,3], Lauren M. Stein[1], Andrew E. Weller[1], Glenn A. Doyle[1], Gabriella Arauco-Shapiro[1], Thomas N. Ferraro[2], Matthew R. Hayes[1], and Wade H. Berrettini[1]

[1] Department of Psychiatry, Perelman School of Medicine, University of Pennsylvania, Philadelphia, Pennsylvania. [2] Department of Biomedical Sciences, Cooper Medical School of Rowan University, Camden, NJ. [3] These authors contributed equally.

***Corresponding author**

Benjamin C. Reiner, PhD

125 S. 31st St., room 2208-1

Philadelphia, PA 19104

Office: (215)-573-0278

Email: bcreiner@pennmedicine.upenn.edu

Abstract

Transcriptomic studies of bulk neural tissue homogenates from persons with schizophrenia and controls have identified differential expressed genes in multiple brain regions. However, the heterogeneous nature prevents identification of relevant cell types. This study utilized single-nuclei transcriptomics of ~311,000 nuclei from frozen human postmortem dorsolateral prefrontal cortex samples from individuals with schizophrenia (n = 14) and controls (n = 16). 2,846 differential expression events were identified in 2,195 unique genes in 19 of 24 transcriptomically-distinct cell populations. ~97% of differential expressed genes occurred in five neuronal cell types, with ~63% occurring in a subtype of PVALB+ inhibitory neurons and HTR2C+ layer V excitatory neurons. Differential expressed genes were enriched for genes associated with schizophrenia GWAS loci and cluster-specific changes in canonical pathways, upstream regulators and causal networks were identified. These results demonstrate cell type specific changes in the context of schizophrenia.

Introduction

Schizophrenia is a chronic psychotic illness affecting ~1% of the population worldwide. With typical onset in late adolescence or early adulthood and a chronic unremitting course, schizophrenia is a devastating disease (reviewed[1]). The heritability of schizophrenia has been estimated at 64%[2] and substantial efforts have been dedicated to identifying genetic variants that are associated with vulnerability to developing the disorder. The largest genome wide association study (GWAS) identified 108 genomic loci associated with schizophrenia[3], and when combined with an additional dataset, subsequent meta-analysis identified 145 genomic loci[4]. Additionally, rare structural variants, such as microdeletions and copy number variants contribute to the heritability of schizophrenia[5-7]. However, these and other studies have only been able to explain a portion of the heritability of schizophrenia, suggesting that gene by environment interactions may play an important role[8]. Supporting this interpretation is

accumulating evidence that demonstrates increased risk for developing schizophrenia is associated with maternal infection and obstetrics complications, early life trauma and social adversity, urbanicity, and substance abuse (reviewed[9]). While these studies have helped elucidate the genetic and environmental components of risk for developing schizophrenia, determining the underlying mechanisms has proven difficult. One approach to identifying the mechanisms that underly schizophrenia is transcriptomics.

Transcriptomic studies utilizing bulk homogenates of frozen human postmortem brain tissue from persons with schizophrenia and controls have identified differentially expressed genes (DEGs) in the amygdala[10], hippocampus[11, 12], superior temporal gyrus[13], anterior cingulate cortex[14, 15], and dorsolateral prefrontal cortex (dlPFC)[16, 17], with the largest of these studies identifying ~700 DEGs in the dlPFC[17]. However, the heterogenous cellular composition of the bulk homogenates prevents identification of the specific cell types in which relevant genes are differentially regulated and expressed. To address these limitations, studies used laser capture microdissection followed with transcriptome analysis by microarray to elucidate the effect of schizophrenia on the transcriptome of individual neural cell types. Examination of layer III and V pyramidal neurons in the dlPFC identified ~1,400 DEGs[18] in the context of schizophrenia, whereas a study of parvalbumin positive (PVALB+) interneurons in the dlPFC identified ~900 DEGs[19]. A substantial portion of the DEGs identified in these studies were unappreciated in previous examinations of bulk homogenates of the same brain regions, supporting more targeted approaches[18, 19]. These findings suggest that examination of transcriptome changes associated with schizophrenia at the level of neural cellular populations is necessary to fully appreciate the differences in cell type specific transcript levels. However, laser capture microdissection studies of human postmortem brain tissue are limited by the ability to examine a small number of cell types in a targeted fashion, rather than the broader cellular landscape of the brain, the relative low throughput of the technique, and the pooling of cells,

which loses the variability of the transcriptome between cells and may collapse transcriptomically-distinct cellular subpopulations.

Recent advances in single nuclei RNA sequencing (snRNAseq) allow for simultaneous transcriptomic profiling of thousands of nuclei, across all neural cell types in frozen human postmortem brain homogenate, with simultaneous indexing of transcripts at the sample, nucleus, and individual transcript level (unique molecular identifier, UMI). The utility of this approach for human postmortem study is supported by evidence suggesting that single cells and their nuclei have similar transcriptomes, with ~98% of transcripts having the same relative levels[20]. snRNAseq has identified cell type-specific transcriptomic changes in human postmortem brain samples from Alzheimer's disease[21], autism[22], multiplesclerosis[23], and major depressive disorder[24].

In this study, we performed snRNAseq of ~311,000 nuclei from dlPFC of individuals with schizophrenia (n = 14) and controls (n = 16). We chose to examine the dlPFC due to the evidence of dlPFC dysfunction in schizophrenia[25]. We identified 2,195 DEGs in 19 of 24 transcriptomically-distinct cell populations. ~97% of the DEGs occurred in five neuronal cell types, with a subtype of PVALB+ inhibitory neurons and 5-Hydroxytryptamine Receptor 2C positive (HTR2C+) layer V excitatory neurons accounting for ~63% of DEGs. The DEGs were enriched for genes associated with schizophrenia GWAS loci and overrepresented in gene ontologies previously associated with the pathophysiology of schizophrenia. Canonical pathway analysis identified cluster-specific alterations in metabolic and cell signaling pathways, and upstream regulator and causal network analysis identified cluster-specific effects of shared DEG regulators. Taken together, the results of this study help elucidate the cell type specific transcriptomic and neurobiological changes that underlie schizophrenia.

Results

Single nuclei RNA sequencing and identification of cell types

To better understand the effects of schizophrenia on the neural transcriptome, we utilized snRNAseq to profile dlPFC nuclei from frozen human postmortem brain samples from 14 individuals with schizophrenia and 16 controls (Supplementary Table 1). Schizophrenia and control groups did not differ in age, postmortem interval, or pH (Supplementary Fig. 1). Tissue samples from the 30 participants were processed to generate nuclei suspensions, which were utilized for snRNAseq using version 3.0 of 10x Genomics 3' gene expression assay. After sequencing to an average depth of ~497 million reads per sample, we initially identified a total of 411,171 nuclei with medians of ~2,895 genes and ~6,588 UMI per nucleus (Supplementary Table 2). The number of sequencing reads per sample, nuclei per sample, average sequencing reads per nuclei per sample, median genes per nuclei per sample, and median UMI per nuclei per sample was consistent between the schizophrenia and control groups (Supplementary Fig. 2). After quality controls (Methods), we identified 311,297 high confidence nuclei, with 149,943 from control samples and 161,354 from schizophrenia samples. These nuclei were used for all further analyses.

To identify nuclei from transcriptomically-distinct cellular populations we used the snRNAseq counts for nuclei from all individuals to perform unbiased clustering using Seurat (Methods). 24 distinct cellular clusters were identified (Fig. 1a). Nuclei from the schizophrenia and control groups were found in all clusters (Fig. 1a), with nuclei from individual samples contributing across the range of most clusters (Supplementary Table 3). Clusters were annotated by expression of known markers for cellular types and all major neural cell types were identified, including inhibitory neurons (InNeuro), excitatory neurons (ExNeuro), oligodendrocytes (Oligo), oligodendrocyte precursor cells (OPC), astrocytes (Astro), microglia (Micro), and endothelial cells (Endo; Fig. 1a-b and Supplementary Fig. 3a). While the number of

nuclei from each major cell type varied by sample, the total number of nuclei from each major cell type was consistent between schizophrenia and control groups (Supplementary Fig. 3b-c and Supplementary Table 3). ExNeuro clusters were further annotated using known markers of the different cortical layers. Populations of layer II/III CUX2+ (ExNeuro4 and ExNeuro5), layer V HTR2C+ (ExNeuro1), layer V SULF2+ (ExNeuro7), layer V KCNK2+ (ExNeuro2 and ExNeuro8), layer V/VI RXFP1+ (ExNeuro3 and ExNeuro6) and layer VI NR4A2+ (ExNeuro9) excitatory neurons were identified (Fig. 1c). Similarly, InNeuro clusters were annotated using genes associated with known subpopulations. Somatostatin positive (SST+, InNeuro1 and InNeuro7), vasoactive intestinal peptide positive (VIP+, InNeuro6), and PVALB+ positive (InNeuro2 and InNeuro3) inhibitory neurons were identified (Fig. 1d).

Differential expression

Cell type specific changes in nuclear transcript levels were compared between the schizophrenia and control groups using the hurdle model, a linear mixed model (LMM), in MAST. A total of 2,846 differential expression events were identified in 2,195 unique DEGs (q-value < 0.1; expression change ≥10%; Supplementary Table 4). DEGs were detected in 19 of the 24 cellular clusters (Fig. 2a), with 48% and 51% of the differential expression events occurring in the InNeuro and ExNeuro major cell types, respectively (Fig. 2b. and Supplementary Table 5). No DEGs were detected in the OPC and Micro cell types and only a single unique DEG was detected in the Endo cell type (Fig. 2b and Supplementary Table 4). The number of differential expression events per cellular cluster was not related to the number of nuclei per cluster (Supplementary Fig. 4a). Of the unique DEGs, ~97% (2,135/2,195) were detected in five neuronal cell clusters (referred to hereafter collectively as the primary neuronal clusters), with ~63% (1,382/2,195) occurring in just two neuronal cell types, the PVALB+ InNeuro2 and HTR2C+ ExNeuro1 cellular clusters (Fig. 2c). No DEG was differentially expressed in more than five cellular clusters (Supplementary Fig. 4b and Supplementary Table

4). The majority of the differential expression events (~66%) were found to be down regulated in schizophrenia samples compared to controls (Fig. 2a-b, Supplementary Fig. 4c and Supplementary Table 5). To independently validate a portion of the DEGs, RNAscope fluorescence *in situ* hybridization was used to validate select DEGs in the PVALB+ InNeuro2 and HTR2C+ ExNeuro1 clusters.

DEGs associated with GWAS loci

The most recent schizophrenia GWAS metanalysis identified 145 genomic loci associated with schizophrenia[4]. The LMM analyzed a total of 12,239 genes, of which 330 were associated with these GWAS loci. 67 of the 2,195 DEGs identified in this analysis overlapped GWAS loci, representing a total of 44 unique loci (Supplementary Table 6). This number of genes represents an ~13% enrichment over what would be expected by chance (hypergeometric test, $p = 0.029$). DEGs associated with schizophrenia GWAS loci were only present in nine clusters. Cluster specific hypergeometric tests identified significant overrepresentation of GWAS-associated genes in DEGs from InNeuro5 (~90%), ExNeuro1 (~32%), and InNeuro2 (~23%) (Fig. 3a and Supplementary Table 7). These results suggest that a fraction of the DEGs identified in this study may represent the transcriptomic changes that underlie specific schizophrenia-associated GWAS loci.

Gene Ontologies and KEGG pathways

To understand the neurobiological consequences of the DEGs in the primary neuronal clusters, DAVID was used to identify gene ontologies (Supplementary Tables 8-22) and KEGG pathways (Supplementary Tables 23-27) in which the DEGs from each cellular cluster were overrepresented. The gene ontology analysis identified cluster-specific overrepresentation of DEGs in ontologies currently believed to be related to the pathophysiology of schizophrenia, such as the biological processes “RNA splicing” and “aerobic respiration” and the cellular

compartments “lysosomal membrane” and “mitochondrion”. Similarly, the KEGG pathway analysis identified overrepresentation DEGs in the KEGG pathways “Spliceosome”, “Oxidative phosphorylation” and “Synaptic vesicle cycle”. Taken together, these suggests that the cluster-specific DEGs may, at least in part, represent a portion of the neurobiological changes that underly schizophrenia-associated neuropathophysiology.

Canonical Pathways

To better identify the metabolic and cell signaling pathways that are likely to be altered in the primary neuronal clusters in the context of schizophrenia, canonical pathway analysis was performed using the DEGs occurring in each of the primary neuronal clusters using Ingenuity Pathway Analysis (IPA). Shared and unique effected canonical pathways were identified for the primary neuronal clusters. The top six shared canonical pathways for the primary neuronal clusters, as determined by IPA activation z-score, a prediction of the direction and magnitude of dysfunction, are presented in Fig. 3b and the top six canonical pathways from each of the primary neuronal clusters, as determined by -log(p-value), are presented in Supplementary Table 28. Given that the majority of DEGs only occurred in the ExNeuro1 and InNeuro2 cellular clusters, shared canonical pathways for these clusters were also determined (Fig. 3c). Interestingly, while some clusters shared predicted directions of effect for some pathways, the DEGs underlying the effect for each cellular cluster was a combination of both shared and unique DEGs (Supplementary Table 28). For example, function of the Oxidative Phosphorylation canonical pathway is predicted to be substantially downregulated in schizophrenia in the ExNeuro1 (z-score = -4.146, p-value = 3.98e-11) and InNeuro2 (z-score = -3.742, p-value = 3.52e-4) cellular clusters (Fig. 3c). Examination of the DEG heat map (Fig. 3d) and signaling pathway (Supplementary Figure 5) for the Oxidative Phosphorylation canonical pathway show a combination of both multi-cluster and cluster-specific DEGs contributing to the overall dysregulation. While the overall results of the canonical pathway analysis suggest that

the primary neuronal clusters share alterations in neurobiologically relevant metabolic and cell signaling pathways in the context of schizophrenia, with respect to both direction and magnitude of effect, examination of the underlying changes suggests that it is actually a combination of shared and cluster-specific alterations of the transcriptome that drive overall pathway dysfunction.

Upstream Regulators of DEGs

The majority of DEGs were only detected in the ExNeuro1 and InNeuro2 cellular clusters, suggesting the possibility that there may be cell type-specific upstream regulators of DEGs unique to these cellular clusters. We utilized IPA to identify putative upstream regulators of DEGs and identified 52 predicted upstream regulators of DEGs for the ExNeuro1 cluster and 87 for the InNeuro2 cluster (Supplementary Tables 29-30). The top six shared upstream regulators of DEGs, as determined by IPA activation z-score, are presented in Fig. 3e. Predicted upstream regulators with the three highest and lowest activation z-scores for the ExNeuro1 and InNeuro2 cellular clusters are displayed in Fig. 3f-g. Similar to the canonical pathways, upstream regulators predicted to be involved in the function of both the ExNeuro1 and InNeuro2 cellular clusters demonstrate both shared and unique DEG targets. For example, the function of the transcription factor NFE2L2, was predicted to be substantially downregulated in both the ExNeuro1 (z-score = -3.747, p-value = 2.54e-2) and InNeuro2 (z-score = -2.659, p-value = 7.64e-3) cellular clusters (Fig. 3e-g and Supplementary Tables 29-30), with 9 shared DEGs out of the 23 and 32 downstream DEG targets, respectively (Supplementary Fig. 6a-b). These results suggest that the shared predicted upstream regulators identified in this analysis may act in a cellular cluster-specific fashion to regulate the DEGs. Supporting the validity of the upstream regulator analysis, 8 DEGs in the ExNeuro1 cluster and 13 DEGs in the InNeuro2 cluster were predicted to be upstream regulators of other DEGs in their respective clusters. All 21 upstream DEGs had altered transcription in the predicted direction of effect (Supplementary

Table 31). In total, these results suggest that the predicted upstream regulators identified in this analysis may play a role in regulating cluster-specific DEGs in the context of schizophrenia.

Causal Networks of DEG regulation

Knowing that regulation of DEGs in the ExNeuro1 and InNeuro2 cellular clusters would not be limited to only direct upstream regulators, we utilized IPA to predict upstream causal networks that putatively regulate the DEGs. The analysis identified 788 and 622 predicted causal networks that regulate the DEGs in the ExNeuro1 and InNeuro2 cellular clusters, respectively (Supplementary Tables 32-33). The top six shared causal network master regulators, as determined by IPA activation z-score, are presented in Fig. 4a. Predicted causal network master regulators with the three highest and lowest activation z-scores for the ExNeuro1 and InNeuro2 cellular clusters are displayed in Fig. 4b-c. Similar to the upstream regulators, there are both shared and cluster-specific DEG targets associated with causal network master regulators predicted to be involved in both the ExNeuro1 and InNeuro2 cellular clusters (Supplementary Tables 32-33). The validity of causal network analysis is supported by the prediction of 32 DEGs in the ExNeuro1 cluster and 30 DEGs in the InNeuro2 cluster as causal network master regulators (Supplementary Tables 32-33). For example, in the ExNeuro1 cluster, *ST3GAL5* was predicted to be an upregulated causal network master regulator that acted through four known regulatory targets and caused the observed downregulation of 25 DEGs (Fig. 4d). In agreement with this prediction, *ST3GAL5* was upregulated ~19% in the ExNeuro1 cluster. Taken together, these results suggest that at least a portion of the predicted master regulators identified in the causal network analysis may be important regulatory elements that control cell cluster-specific transcriptomic changes in the context of schizophrenia.

References

1. Owen, M.J., Sawa, A. & Mortensen, P.B. Schizophrenia. *Lancet* **388**, 86-97 (2016).
2. Lichtenstein, P.*, et al.* Common genetic determinants of schizophrenia and bipolar disorder in Swedish families: a population-based study. *Lancet* **373**, 234-239 (2009).
3. Schizophrenia Working Group of the Psychiatric Genomics, C. Biological insights from 108 schizophrenia-associated genetic loci. *Nature* **511**, 421-427 (2014).
4. Pardinas, A.F.*, et al.* Common schizophrenia alleles are enriched in mutation-intolerant genes and in regions under strong background selection. *Nature genetics* **50**, 381-389 (2018).
5. Stefansson, H.*, et al.* Large recurrent microdeletions associated with schizophrenia. *Nature* **455**, 232-236 (2008).
6. Walsh, T.*, et al.* Rare structural variants disrupt multiple genes in neurodevelopmental pathways in schizophrenia. *Science* **320**, 539-543 (2008).
7. Xu, B.*, et al.* Strong association of de novo copy number mutations with sporadic schizophrenia. *Nature genetics* **40**, 880-885 (2008).
8. van Os, J., Rutten, B.P. & Poulton, R. Gene-environment interactions in schizophrenia: review of epidemiological findings and future directions. *Schizophr Bull* **34**, 1066-1082 (2008).
9. Stilo, S.A. & Murray, R.M. Non-Genetic Factors in Schizophrenia. *Curr Psychiatry Rep* **21**, 100 (2019).
10. Chang, X.*, et al.* RNA-seq analysis of amygdala tissue reveals characteristic expression profiles in schizophrenia. *Transl Psychiatry* **7**, e1203 (2017).
11. Hwang, Y.*, et al.* Gene expression profiling by mRNA sequencing reveals increased expression of immune/inflammation-related genes in the hippocampus of individuals with schizophrenia. *Transl Psychiatry* **3**, e321 (2013).
12. Kohen, R., Dobra, A., Tracy, J.H. & Haugen, E. Transcriptome profiling of human hippocampus dentate gyrus granule cells in mental illness. *Transl Psychiatry* **4**, e366 (2014).
13. Wu, J.Q.*, et al.* Transcriptome sequencing revealed significant alteration of cortical promoter usage and splicing in schizophrenia. *PloS one* **7**, e36351 (2012).
14. Zhao, Z.*, et al.* Transcriptome sequencing and genome-wide association analyses reveal lysosomal function and actin cytoskeleton remodeling in schizophrenia and bipolar disorder. *Molecular psychiatry* **20**, 563-572 (2015).
15. Hong, S., Chen, X., Jin, L. & Xiong, M. Canonical correlation analysis for RNA-seq co-expression networks. *Nucleic acids research* **41**, e95 (2013).
16. Fillman, S.G.*, et al.* Increased inflammatory markers identified in the dorsolateral prefrontal cortex of individuals with schizophrenia. *Molecular psychiatry* **18**, 206-214 (2013).
17. Fromer, M.*, et al.* Gene expression elucidates functional impact of polygenic risk for schizophrenia. *Nat Neurosci* **19**, 1442-1453 (2016).
18. Arion, D.*, et al.* Transcriptome Alterations in Prefrontal Pyramidal Cells Distinguish Schizophrenia From Bipolar and Major Depressive Disorders. *Biol Psychiatry* **82**, 594-600 (2017).
19. Enwright Iii, J.F.*, et al.* Transcriptome alterations of prefrontal cortical parvalbumin neurons in schizophrenia. *Molecular psychiatry* **23**, 1606-1613 (2018).
20. Grindberg, R.V.*, et al.* RNA-sequencing from single nuclei. *Proceedings of the National Academy of Sciences of the United States of America* **110**, 19802-19807 (2013).
21. Mathys, H.*, et al.* Single-cell transcriptomic analysis of Alzheimer's disease. *Nature* **570**, 332-337 (2019).
22. Velmeshev, D.*, et al.* Single-cell genomics identifies cell type-specific molecular changes in autism. *Science* **364**, 685-689 (2019).

23. Schirmer, L., *et al.* Neuronal vulnerability and multilineage diversity in multiple sclerosis. *Nature* **573**, 75-82 (2019).
24. Nagy, C., *et al.* Single-nucleus transcriptomics of the prefrontal cortex in major depressive disorder implicates oligodendrocyte precursor cells and excitatory neurons. *Nat Neurosci* **23**, 771-781 (2020).
25. Hoftman, G.D., Datta, D. & Lewis, D.A. Layer 3 Excitatory and Inhibitory Circuitry in the Prefrontal Cortex: Developmental Trajectories and Alterations in Schizophrenia. *Biol Psychiatry* **81**, 862-873 (2017).

Figure Legends

Fig. 1 | snRNAseq and clustering. a, The transcriptome profile of ~311,000 nuclei were utilized for unbiased clustering (dendrogram) and the resulting clusters were annotated with genes known to be markers for major neural cell types (dot plot, cell types and their respective markers are color coded). The size and color of dots is proportional to the percentage of cells expressing the gene (Pct. Exp.) and the average expression level of the gene (Avg. Exp.), respectively. The number columns list number of nuclei from the control (CT) and schizophrenia (SZ) groups that are present in each cluster. The bar graph depicts the average number of unique molecular identifiers (UMI) per nucleus for each cluster. InNeuro, inhibitory neuron; ExNeuro, excitatory neuron; Oligo, oligodendrocyte; OPC, oligodendrocyte precursor cell; Astro, astrocyte; Endo, endothelial cell; Micro, microglia/macrophages. **b,** A uniform manifold approximation and projection (UMAP) dimension reduction plot of all nuclei color coded by major neural cell type. **c,** Excitatory neuron clusters were annotated with known markers of cortical layer II/III (CUX2), layer V (HTR2C, SULF2, KCNK2 and PCP4), layer V/VI (RXFP1), and layer VI (NR4A2) to determine the cortical layer represented by each excitatory neuron cluster. **d,** Inhibitory neuron clusters were annotated using known markers of inhibitory neuron subtypes, including calcium binding proteins (PVALB, CALB1, and CALB2), neuropeptides

(SST, VIP, and CCK), and other known markers of cortical inhibitory neurons (GAD1, GAD2, RELN, and NOS1).

Fig. 2 | Differential expression. a, A categorical scatter plot depicting the $\log_2$ fold change of all differential expression events. Dashed lines indicate the minimum bioinformatic cutoff of 10% change in gene expression. This figure is depicted with a continuous y-axis in Supplementary Fig. 4b. **b,** The number of differential expression events per major cell type. **c,** UpSet plot of the number of unique DEGs that are unique or shared between the five neuronal cell cluster that encompass the majority (~97%) of all DEGs.

Fig. 3 | Functional correlations of DEGs. a, Hypergeometric test p-values for cluster specific overlap between DEGs associated with individual cellular clusters and genes associated with the schizophrenia GWAS loci. **b & c,** Canonical pathways predicted to be disrupted in the (b) primary neuronal clusters and in the (c) ExNeuro1 and InNeuro2 cellular clusters, ranked by absolute magnitude of IPA activation z-score, showing multi-cluster and cluster-specific directions of effect. **d,** DEGs associated with disruption of the oxidative phosphorylation canonical pathway. **e,** Shared predicted upstream regulators of DEGs, ranked as in (c). **f & g,** Predicted upstream regulators in the (f) ExNeuro1 and (g) InNeuro2 cellular clusters with the three highest and lowest predicted activation z-scores.

Fig. 4 | Causal networks. a, Shared predicted causal network master regulators of DEGs, in the ExNeuro1 and InNeuro2 cellular clusters, ranked by absolute magnitude of IPA activation z-score. **b & c,** Predicted causal network master regulators of DEGs in the (b) ExNeuro1 and (c) InNeuro2 cellular clusters with the three highest and lowest predicted activation z-scores. **d,** The predicted causal network of ST3GAL5 in ExNeuro1. Based on the 25 downregulated DEGs

(green), it was predicted that the function of ST3GAL5 was upregulated (red) and acted through the predicted intermediates (white). ST3GAL5 was upregulated in the ExNeuro1 cluster.

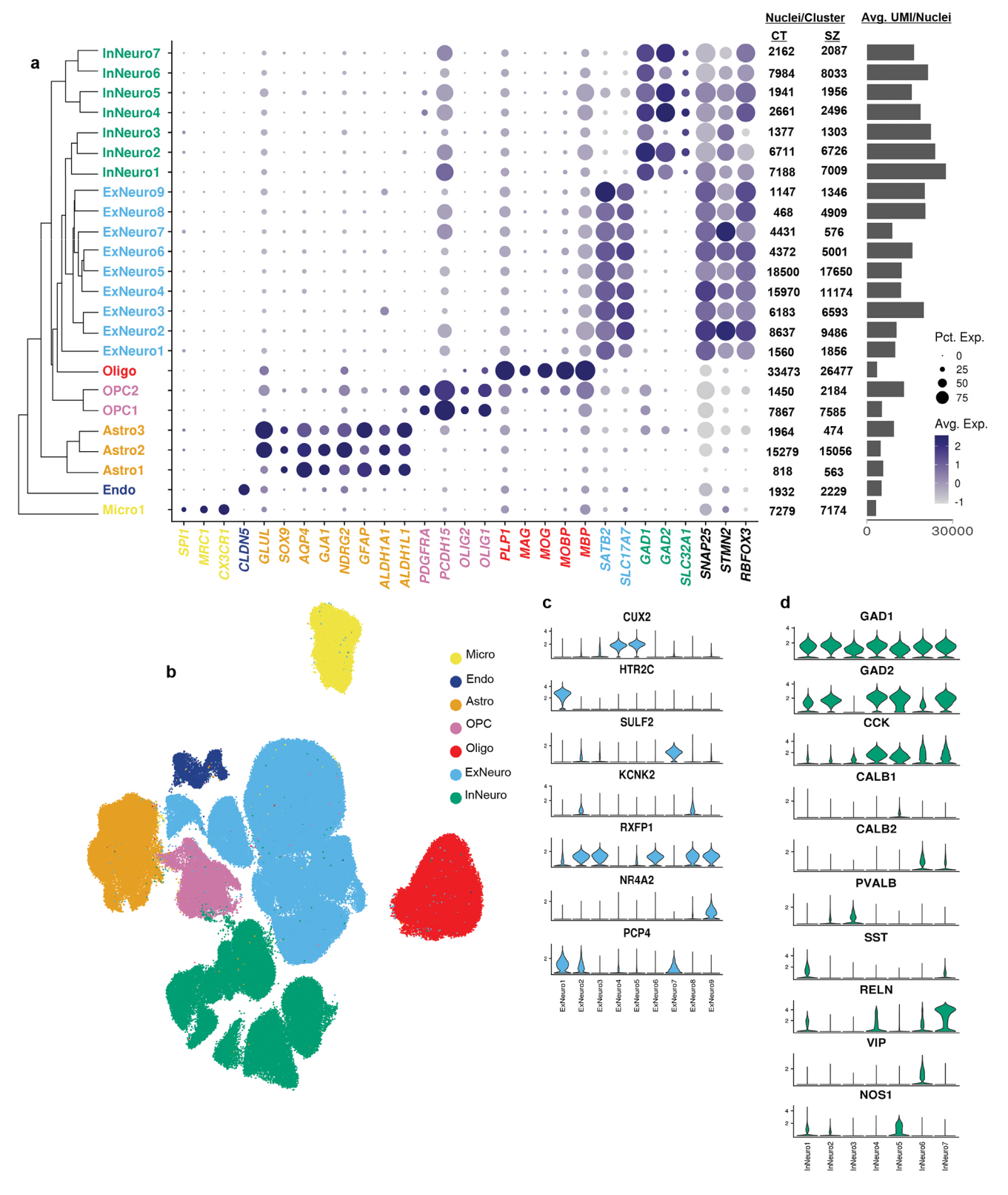
a
Nuclei/Cluster
CT
SZ
Avg. UMI/Nuclei
InNeuro7 2162 2087
InNeuro6 7984 8033
InNeuro5 1941 1956
InNeuro4 2661 2496
InNeuro3 1377 1303
InNeuro2 6711 6726
InNeuro1 7188 7009
ExNeuro9 1147 1346
ExNeuro8 468 4909
ExNeuro7 4431 576
ExNeuro6 4372 5001
ExNeuro5 18500 17650
ExNeuro4 15970 11174
ExNeuro3 6183 6593
ExNeuro2 8637 9486
ExNeuro1 1560 1856
Oligo 33473 26477
OPC2 1450 2184
OPC1 7867 7585
Astro3 1964 474
Astro2 15279 15056
Astro1 818 563
Endo 1932 2229
Micro1 7279 7174
SPI1 MRC1 CX3CR1 CLDN5 GLUL SOX9 AQP4 GJA1 NDRG2 GFAP ALDH1A1 ALDH1L1 PDGFRA PCDH15 OLIG2 OLIG1 PLP1 MAG MOG MOBP MBP SATB2 SLC17A7 GAD1 GAD2 SLC32A1 SNAP25 STMN2 RBFOX3
Pct. Exp.
0
25
50
75
Avg. Exp.
2
1
0
-1
0
30000
b
Micro
Endo
Astro
OPC
Oligo
ExNeuro
InNeuro
c
CUX2
HTR2C
SULF2
KCNK2
RXFP1
NR4A2
PCP4
ExNeuro1 ExNeuro2 ExNeuro3 ExNeuro4 ExNeuro5 ExNeuro6 ExNeuro7 ExNeuro8 ExNeuro9
d
GAD1
GAD2
CCK
CALB1
CALB2
PVALB
SST
RELN
VIP
NOS1
InNeuro1 InNeuro2 InNeuro3 InNeuro4 InNeuro5 InNeuro6 InNeuro7

b

	Up	Down
InNeuro	411	946
ExNeuro	523	941
Oligo	18	0
OPC	0	0
Astro	4	2
Endo	1	0
Micro	0	0
Total	957	1889

c

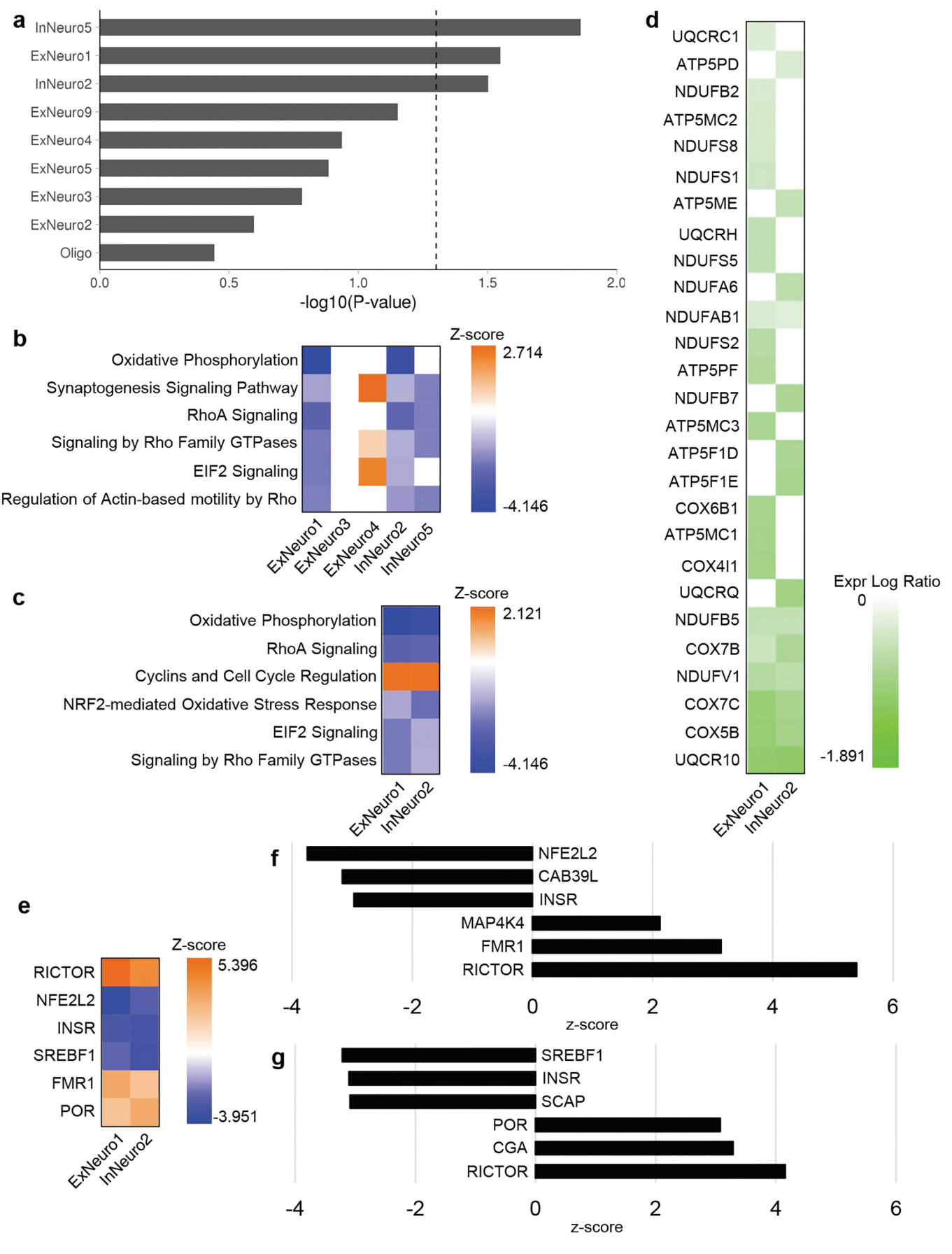
a
InNeuro5
ExNeuro1
InNeuro2
ExNeuro9
ExNeuro4
ExNeuro5
ExNeuro3
ExNeuro2
Oligo
0.0
0.5
1.0
1.5
2.0
-log10(P-value)
b
Z-score
2.714
-4.146
Oxidative Phosphorylation
Synaptogenesis Signaling Pathway
RhoA Signaling
Signaling by Rho Family GTPases
EIF2 Signaling
Regulation of Actin-based motility by Rho
ExNeuro1
ExNeuro3
ExNeuro4
InNeuro2
InNeuro5
c
Z-score
2.121
-4.146
Oxidative Phosphorylation
RhoA Signaling
Cyclins and Cell Cycle Regulation
NRF2-mediated Oxidative Stress Response
EIF2 Signaling
Signaling by Rho Family GTPases
ExNeuro1
InNeuro2
d
UQCRC1
ATP5PD
NDUFB2
ATP5MC2
NDUFS8
NDUFS1
ATP5ME
UQCRH
NDUFS5
NDUFA6
NDUFAB1
NDUFS2
ATP5PF
NDUFB7
ATP5MC3
ATP5F1D
ATP5F1E
COX6B1
ATP5MC1
COX4I1
UQCRQ
NDUFB5
COX7B
NDUFV1
COX7C
COX5B
UQCR10
Expr Log Ratio
0
-1.891
ExNeuro1
InNeuro2
e
Z-score
5.396
-3.951
RICTOR
NFE2L2
INSR
SREBF1
FMR1
POR
ExNeuro1
InNeuro2
f
NFE2L2
CAB39L
INSR
MAP4K4
FMR1
RICTOR
-4
-2
0
2
4
6
z-score
g
SREBF1
INSR
SCAP
POR
CGA
RICTOR
-4
-2
0
2
4
6
z-score

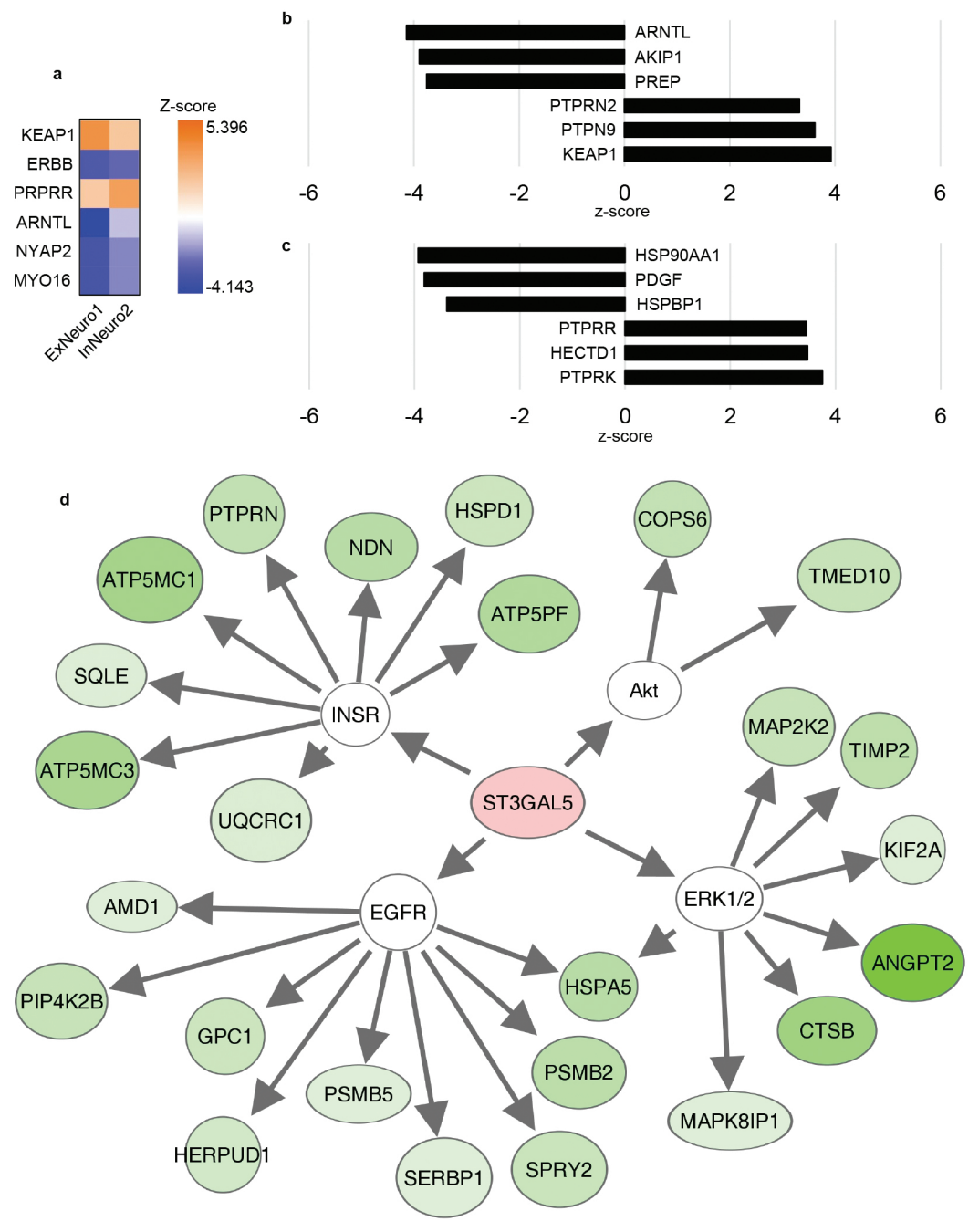
a
Z-score
5.396
-4.143
KEAP1
ERBB
PRPRR
ARNTL
NYAP2
MYO16
ExNeuro1
InNeuro2
b
ARNTL
AKIP1
PREP
PTPRN2
PTPN9
KEAP1
-6
-4
-2
0
2
4
6
z-score
c
HSP90AA1
PDGF
HSPBP1
PTPRR
HECTD1
PTPRK
-6
-4
-2
0
2
4
6
z-score
d
PTPRN
NDN
HSPD1
COPS6
ATP5MC1
ATP5PF
TMED10
SQLE
INSR
Akt
MAP2K2
TIMP2
ATP5MC3
UQCRC1
ST3GAL5
KIF2A
AMD1
EGFR
ERK1/2
ANGPT2
PIP4K2B
HSPA5
CTSB
GPC1
PSMB2
PSMB5
MAPK8IP1
HERPUD1
SERBP1
SPRY2